

**VIRTUAL EFFECTS OF PHYSICS BEYOND THE STANDARD
MODEL * †**

J.L. HEWETT

Stanford Linear Accelerator Center, Stanford University, Stanford, CA 94309, USA

ABSTRACT

We examine the indirect effects of new physics on a variety of processes in the B system, such as the $Z \rightarrow b\bar{b}$ vertex, the decays $B \rightarrow X_s\gamma$ and $B \rightarrow X_s\ell^+\ell^-$, and CP violation.

1. Introduction

The investigation of virtual effects of new physics provides an important opportunity to probe the presence of interactions beyond the Standard Model (SM). Various types of experiments may expose the existence of new physics, including the search for direct production of new particles at high energy accelerators. Although this scenario has the advantage in that it would yield the cleanest observation of new physics, it is limited by the kinematic reach of colliders. A complementary approach is offered by examining the indirect effects of new interactions in higher order processes, such as rare or forbidden decays and precision electroweak measurements, and testing for deviations from SM predictions. In fact, studies of new loop induced couplings can provide a means of probing the detailed structure of the SM at the level of radiative corrections where Glashow-Iliopoulos-Maiani (GIM) cancellations are important. In some cases the constraints on new degrees of freedom via indirect effects surpass those obtainable from collider searches. Given the large amount of high luminosity data which will become available during the next decade, precision measurements and rare processes will play a major role in the search for physics beyond the SM. Here we highlight the importance of virtual effects in the B system, focusing on two-Higgs-doublet models, supersymmetry, and models with anomalous couplings.

2. The $Z \rightarrow b\bar{b}$ Vertex

The SM continues to provide an excellent description of precision electroweak data,¹ especially in the light of the discovery of the top-quark² in the mass range predicted by this data. The only hint of a potential discrepancy is a mere $(2 - 2.5)\sigma$ deviation from SM expectations for the quantity $R_b \equiv \Gamma(Z \rightarrow b\bar{b})/\Gamma(Z \rightarrow \text{hadrons})$. A global fit to all LEP data gives the result¹ $R_b = 0.2204 \pm 0.0020$. In this fit, the

*Work Supported by the Department of Energy, Contract DE-AC03-76SF00515

†Presented at the *4th International Conference on Physics Beyond the Standard Model*, Lake Tahoe, CA, December 13-18, 1994

value of R_b is highly correlated to the value of the corresponding quantity R_c , which is measured to be $R_c = 0.1606 \pm 0.0095$. If R_c is fixed to its SM value of 0.171, the LEP result for R_b becomes 0.2196 ± 0.0019 . In the SM, R_b is sensitive to additional vertex corrections involving the top-quark, while the remaining electroweak and QCD radiative corrections largely cancel in the ratio. These additional vertex corrections suppress $\Gamma(Z \rightarrow b\bar{b})$ by an amount which is approximately quadratic in the top-quark mass and hence reduce the value of R_b for the measured range of m_t . This can be seen explicitly in Fig. 1(a) from Grant,³ where the solid curves compare R_b in the SM (taking $m_h = 100$ GeV) with the corresponding quantity R_d which is not affected by this top-quark vertex correction. Using ZFITTER4.9⁴ we find $R_b = 0.2157$, taking $m_t = 175$ GeV (and $m_h = 300$ GeV, $\alpha_s = 0.125$).

We first consider the effects of an enlarged Higgs sector on R_b . We examine a two-Higgs-doublet model (denoted⁵ as Model II) which naturally avoids tree-level flavor-changing neutral currents, and where the second doublet, ϕ_2 , gives mass to the up-type quarks, while the down-type quarks and charged leptons receive their mass from ϕ_1 . Each doublet obtains a vacuum expectation value (vev) v_i , subject to the constraint that $v_1^2 + v_2^2 = v^2$, where v is the usual vev present in the SM. The fermionic couplings of the five physical Higgs bosons are summarized in Ref. 5 and are dependent upon the fermion mass, $\tan\beta \equiv v_2/v_1$, and the neutral scalar mixing angle α . Two additional classes of $Zb\bar{b}$ vertex corrections are present in this model^{3,6}; (i) the charged Higgs boson H^\pm being exchanged together with the t-quark, and (ii) the neutral scalar h^0, H^0 and pseudoscalar A^0 Higgs bosons exchanged with the b-quark. The diagrams involving the H^\pm exchange yield negative contributions to $Z \rightarrow b\bar{b}$ and grow as m_t increases, thus further suppressing this width. The contributions from the neutral Higgs exchange can have either sign, depending on the values of the scalar masses (this correction is positive if h^0 and A^0 have small degenerate masses), and become important for large values of $\tan\beta$. This scenario is summarized³ by the dashed curves in Fig. 1(a), where the upper (lower) curves correspond to $\tan\beta = 70(1)$ with $m_{h^0, A^0} = 50$ GeV, $m_{H^0} = 875$ GeV, $m_{H^\pm} = 422$ GeV, and $\alpha = \pi/2$. We see that it is possible to accommodate the data in this model for very specific values of the parameters.

The (s)particles present in supersymmetric theories also contribute to the $Zb\bar{b}$ vertex correction. In addition to the SM and Model II charged and neutral Higgs corrections discussed above, there are further contributions from (i) top-squark-chargino and (ii) b-squark-neutralino exchange. These additional corrections have been examined by several authors,^{6,7} and have been found to be sizeable in some regions of the parameter space. In particular, the light \tilde{t}_1 -chargino loops can give large corrections, while the heavy \tilde{t}_2 -chargino and \tilde{b} -neutralino corrections decouple. Wells *et al.*,⁷ have performed a phenomenological analysis of these supersymmetric corrections and established that consistency at the 1σ level with the LEP data on R_b , together with the measured value of m_t , requires light sparticles. Specifically, they find the constraint $m_{\tilde{\chi}_1^\pm} < 85$ GeV and $m_{\tilde{t}_1} < 100$ GeV with $\min(\tilde{\chi}_1^\pm, \tilde{t}_1) < 65$ GeV. This is shown explicitly in Fig. 1(b) from this reference.

Anomalous WWZ interactions would impact the top-quark corrections to the $Zb\bar{b}$ vertex. The tri-linear gauge boson vertex can be probed by looking for deviations from the SM in tree-level processes such as $e^+e^- \rightarrow W^+W^-$, or in loop order processes,

for example the $g - 2$ of the muon. In the latter case, cutoffs must be used in order to regulate the divergent loop integrals and can introduce errors by attributing a physical significance to the cutoff.⁸ The CP-conserving interaction Lagrangian for WWV interactions can be written as⁹

$$\begin{aligned} \mathcal{L}_{WWV} = & ig_{WWV} \left[\left(W_{\mu\nu}^\dagger W^\mu V^\nu - W_\mu^\dagger V_\nu W^{\mu\nu} \right) + \kappa_V W_\mu^\dagger W_\nu V^{\mu\nu} + \frac{\lambda_V}{M_W^2} W_{\lambda\mu}^\dagger W_\nu^\mu V^{\nu\lambda} \right. \\ & \left. - ig_5^V \epsilon^{\mu\nu\lambda\rho} \left(W_\mu^\dagger \partial_\lambda W_\nu - W_\nu \partial_\lambda W_\mu^\dagger \right) V_\rho \right], \end{aligned} \quad (1)$$

where $V_{\mu\nu} = \partial_\mu V_\nu - \partial_\nu V_\mu$, $g_{WWV} = gc_w(e)$ for $V_\mu = Z_\mu(A_\mu)$, and the parameters ($\Delta\kappa_V \equiv \kappa_V - 1$) take on the values $\Delta\kappa_V, \lambda_V, g_5^V = 0$ in the SM. Eboli *et al.*,¹⁰ have examined the affect of these anomalous interactions on R_b and derived the 95% C.L. bounds (for $m_t = 175$ GeV), $-1.2 < \Delta\kappa_Z < -0.091$, $-6.0 < \lambda_Z < -0.46$, $-1.9 < g_5^Z < -0.14$, assuming that only one parameter is non-zero at a time, and setting the cutoff scale $\Lambda = 1$ TeV. Negative values of these parameters yield positive shifts in R_b and hence are favored. Note that these parameters must be unnaturally large in order to accommodate the data.

The existence of anomalous couplings between the b-quark and the Z boson could cause a significant shift¹¹ in the value of R_b . The lowest dimensional non-renormalizable operators which can be added to the SM take the form of either electric or magnetic dipole form factors. Defining κ and $\tilde{\kappa}$ as the real parts of the magnetic and electric dipole form factors, respectively, (evaluated at $q^2 = M_Z^2$) the interaction Lagrangian is

$$\mathcal{L} = \frac{g}{2c_w} \bar{b} \left[\gamma_\mu (v_b - a_b \gamma_5) + \frac{i}{2m_b} \sigma_{\mu\nu} q^\nu (\kappa_b^Z - i\tilde{\kappa}_b^Z \gamma_5) \right] b Z^\mu. \quad (2)$$

The influence of these couplings on R_b , as well as the asymmetry parameter A_b , is presented in Fig. 1(c) from Rizzo,¹¹ where the ratio of these quantities calculated with the above Lagrangian to that of the SM (as defined by ZFITTER⁴) is displayed. In this figure the solid (dashed) curves represent the predictions when κ_b^Z ($\tilde{\kappa}_b^Z$) is taken to be non-zero, with the diamonds representing unit steps of 0.01 in these parameters. The data points are also shown, with $m_t = 170$ (dotted), 180 (solid), 190 (dashed) GeV. Note that the present data prefer non-zero values for these couplings.

3. Radiative B Decays

Radiative B decays have become one of the best testing grounds of the SM due to recent progress on both the experimental and theoretical fronts. The CLEO Collaboration has recently reported¹² the observation of the inclusive decay $B \rightarrow X_s \gamma$ with a branching fraction of $(2.32 \pm 0.57 \pm 0.35) \times 10^{-4}$. Observation of this process at the inclusive level removes the uncertainties associated with folding in the imprecisely predicted¹³ ratio of exclusive to inclusive rates when comparing theoretical results with exclusive data. On the theoretical side, the reliability of the calculation of the quark-level process $b \rightarrow s \gamma$ is improving¹⁴ as agreement on the leading-logarithmic QCD corrections has been reached and partial calculations at the next-to-leading logarithmic order are underway. These new results have inspired a large number of investigations of this decay in various classes of models.¹⁵

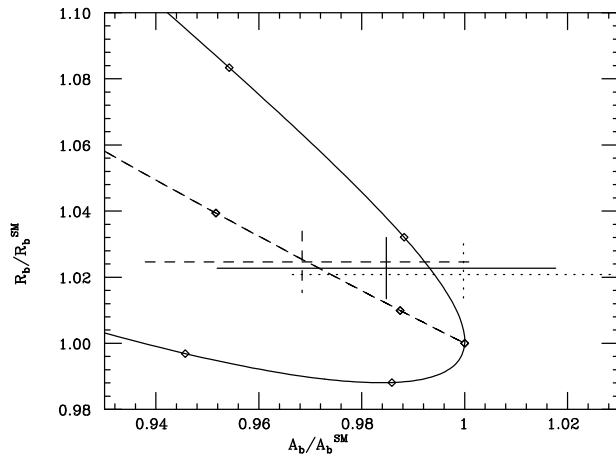


Fig. 1. (a) R_b as a function of the top-quark mass in the SM (solid curves) and in the two-Higgs-doublet Model II (dashed curves) from Ref. 3. The value of the parameters are as described in the text. The error bars indicate the 1σ experimental measurements. (b) Bounds on the lightest chargino and stop-squark masses which are consistent with R_b at the 1σ level from Ref. 7 for $m_t = 157, 174, 191$ GeV. The allowed region lies below the curves. (c) The R_b and asymmetry parameter A_b plane for non-zero values of the electric and magnetic dipole couplings from Rizzo in Ref. 11, where the diamonds represent unit increments in these quantities in steps of 0.01. The error bars represent the data, scaled to the SM prediction with $m_t = 170, 180, 190$ GeV corresponding to the dotted, solid, dashed curves, respectively.

In the SM, the quark-level transition $b \rightarrow s\gamma$ is mediated by W -boson and t -quark exchange in an electromagnetic penguin diagram. To obtain the branching fraction, the inclusive rate is scaled to that of the semi-leptonic decay $b \rightarrow X\ell\nu$. This procedure removes uncertainties from the overall factor of m_b^5 , and reduces the ambiguities involved with the imprecisely determined Cabibbo-Kobayashi-Maskawa (CKM) factors. The result is then rescaled by the experimental value of $B(b \rightarrow X\ell\nu)$. The calculation of $\Gamma(b \rightarrow s\gamma)$ employs the renormalization group evolution¹⁴ for the coefficients of the $b \rightarrow s$ transition operators in the effective Hamiltonian at the leading logarithmic level. The participating operators consist of the current-current operators $O_{1,2}$, the QCD penguin operators O_{3-6} , and the electro- and chromo-magnetic operators $O_{7,8}$. The Wilson coefficients of the $b \rightarrow s$ operators are evaluated perturbatively at the W scale, where the matching conditions are imposed, and evolved down to the renormalization scale μ , usually taken to be $\sim m_b$. This procedure yields the branching fraction $B(b \rightarrow s\gamma) = 2.92_{-0.59}^{+0.77} \times 10^{-4}$ for a top-quark mass of 175 GeV. The central value corresponds to $\mu = m_b$, while the upper and lower errors represent the deviation due to assuming $\mu = m_b/2$ and $\mu = 2m_b$, respectively. We see that (i) this value compares favorably to the recent CLEO measurement and (ii) the freedom of choice in the value of the renormalization scale introduces an uncertainty of order 25%. Clearly, this uncertainty must be taken into account when determining constraints on new physics from this process.

Before discussing explicit models of new physics, we first investigate the constraints placed directly on the Wilson coefficients of the magnetic moment operators. Writing the coefficients at the matching scale in the form $c_i(M_W) = c_i(M_W)_{SM} + c_i(M_W)_{new}$, where $c_i(M_W)_{new}$ represents the contributions from new interactions, we see that the CLEO measurement limits the possible values of $c_i(M_W)_{new}$ for $i = 7, 8$. These bounds are depicted in Fig. 2(a) for $m_t = 175$ GeV, where the allowed regions lie inside the diagonal bands. We note that the two bands occur due to the overall sign ambiguity in the determination of the coefficients (recall that $B(b \rightarrow s\gamma) \propto |c_7^{eff}(\mu)|^2$), and by including the upper and lower CLEO bounds. The horizontal lines correspond to potential limits $B(b \rightarrow sg) < (3-30) \times B(b \rightarrow sg)_{SM}$. We see that such a constraint on $b \rightarrow sg$ is needed to further restrict the values of the Wilson coefficients at the matching scale.

In two-Higgs-doublet models the H^\pm contributes to $b \rightarrow s\gamma$ via virtual exchange together with the top-quark, and the dipole $b \rightarrow s$ operators ($O_{7,8}$) receive contributions from this exchange. At the W scale the coefficients of these operators take the form (in Model II described above)

$$c_i(M_W) = G_i^{SM}(m_t^2/M_W^2) + A_{1_i}^{H^\pm}(m_t^2/m_{H^\pm}^2) + \frac{1}{\tan^2\beta} A_{2_i}^{H^\pm}(m_t^2/m_{H^\pm}^2), \quad (3)$$

where $i = 7, 8$. The analytic form of the functions A_{1_i}, A_{2_i} can be found in Ref. 16. In Model II, large enhancements appear for small values of $\tan\beta$, but more importantly, we see that $B(b \rightarrow s\gamma)$ is always larger than that of the SM, independent of the value of $\tan\beta$ due to the presence of the $A_{1_i}^{H^\pm}$ term. In this case, the CLEO upper bound excludes^{12,17} the region to the left and beneath the curves shown in Fig. 2(b) for $m_t = 174 \pm 16$ GeV and $\mu = 2m_b$.

The H^\pm couplings in Model II are of the type present in Supersymmetry. However, the limits obtained in supersymmetric theories also depend on the size of the other super-particle contributions to $b \rightarrow s\gamma$, and are generally much more complex. In particular, it has been shown^{18,19} that large contributions can arise from stop-squark and chargino exchange (due to the possibly large stop-squark mass splitting), as well as from the gluino and down-type squark loops (due to left-right mixing in the sbottom sector). The additional neutralino-down-squark contributions are expected to be small. Some regions of the parameter space can thus cancel the H^\pm contributions resulting in predictions for the branching fraction at (or even below) the SM value, while other regions always enhance the amplitude. In minimal supergravity models with radiative breaking, the sign of the sparticle loop contributions is found to be correlated with the sign of the higgsino mass parameter μ . This is demonstrated in Fig. 2(c) from Ref. 19, where $B(b \rightarrow s\gamma)$ is displayed as a function of the charged Higgs mass, for negative and positive values of μ . The points in this figure represent a scan of the remaining parameter space that is phenomenologically consistent. We see that taking $\mu < 0$ (> 0) enhances (suppresses) the branching fraction from the predictions in Model II. These authors¹⁹ also find that $m_{H^\pm} > 400$ GeV for $\mu < 0$ and $\tan\beta \geq 10$, while $m_{H^\pm} > 180$ GeV with $3 \leq \tan\beta \leq 5$ for both signs of μ .

The trilinear gauge coupling of the photon to W^+W^- can also be tested in radiative B decays. $b \rightarrow s\gamma$ naturally avoids the problem of introducing cutoffs to regulate the divergent loop integrals due to the cancellations provided by the GIM mechanism, and hence cutoff independent bounds on anomalous couplings can be obtained. In this decay only the coefficient of the magnetic dipole operator, O_7 , is modified by the presence of the additional terms in Eq. (1) and can be written as

$$c_7(M_W) = G_7^{SM}(m_t^2/M_W^2) + \Delta\kappa_\gamma A_1(m_t^2/M_W^2) + \lambda_\gamma A_2(m_t^2/M_W^2). \quad (4)$$

The explicit form of the functions $A_{1,2}$ can be found in Ref. 20. As both of these parameters are varied, either large enhancements or suppressions over the SM prediction for the $b \rightarrow s\gamma$ branching fraction can be obtained. When one demands consistency with both the upper and lower CLEO bounds, a large region of the $\Delta\kappa_\gamma - \lambda_\gamma$ parameter plane is excluded; this is displayed in Fig. 2(d) from Ref. 12 for $m_t = 174$ GeV. Here, the allowed region is given by the cross-hatched area, where the white strip down the middle is excluded by the lower bound and the outer white areas are ruled out by the upper limit on $B(b \rightarrow s\gamma)$. The ellipse represents the region allowed by D0.²¹ Note that the SM point in the $\Delta\kappa_\gamma - \lambda_\gamma$ plane (labeled by the dot) lies in the center of one of the allowed regions. We see that the collider constraints are complementary to those from $b \rightarrow s\gamma$.

4. The Decay $B \rightarrow X_s \ell^+ \ell^-$

The inclusive process $b \rightarrow s \ell^+ \ell^-$ also offers an excellent opportunity to search for new physics. The decay proceeds via electromagnetic and Z penguin as well as by W box diagrams, and hence can probe different coupling structures than the pure electromagnetic process $b \rightarrow s\gamma$. This reaction also receives long distance contributions from the processes $B \rightarrow K^{(*)} \psi^{(\prime)}$ followed by $\psi^{(\prime)} \rightarrow \ell^+ \ell^-$ and from $c\bar{c}$ continuum intermediate states. The short distance contributions lead to the inclusive branching

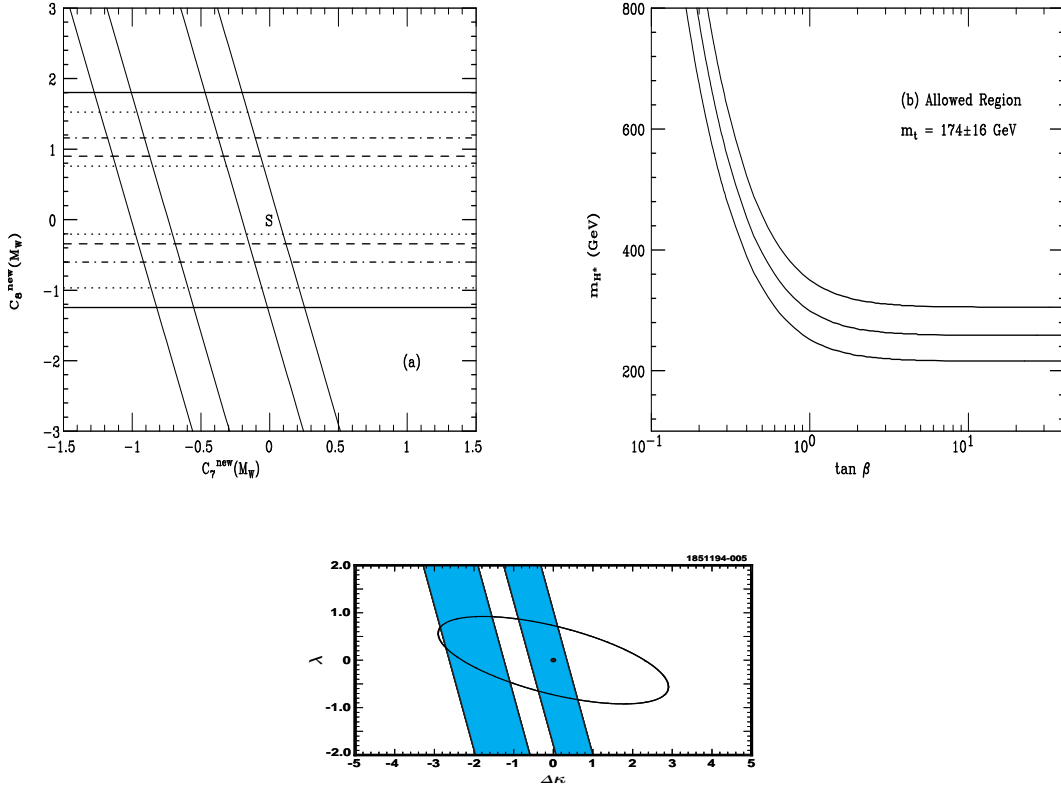


Fig. 2. (a) Bounds on the contributions from new physics to $c_{7,8}$. The region allowed by CLEO corresponds to the area inside the diagonal bands. The horizontal lines represent potential measurements of $R \equiv B(b \rightarrow sg)/B(b \rightarrow sg)_{SM} < 30, 20, 10, 5, 3$ corresponding to the set of solid, dotted, dash-dotted, dashed, and dotted lines, respectively. The point ‘S’ represents the SM. (b) $B(b \rightarrow s\gamma)$ as a function of the charged Higgs mass with $m_t = 175$ GeV and $\tan \beta = 5$ from Ref. 19. The solid curve corresponds to the two-Higgs-doublet Model II value, while the dashed-dot curve represents the SM. The points represent a scan of the supersymmetric parameter space as described in the text. (c) Limits from $b \rightarrow s\gamma$ in the charged Higgs mass - $\tan \beta$ plane. The excluded region is that to the left and below the curves. The three curves correspond to the values $m_t = 190, 174, 158$ GeV from top to bottom. (d) Constraints on anomalous $WW\gamma$ couplings from Ref. 12. The shaded area is that allowed by CLEO and the interior of the ellipse is the region allowed by D0. The dot represent the SM values.

fractions²² (including the leading logarithmic QCD corrections) $B(B \rightarrow X_s \ell^+ \ell^-) \sim (15, 7, 2) \times 10^{-6}$ for $\ell = (e, \mu, \tau)$, respectively, and hence these modes will likely be observed during the next few years. The best method of separating the long and short distance contributions, as well as observing any deviations from the SM, is to measure the various kinematic distributions associated with the final state lepton pair, such as the lepton pair invariant mass distribution,²² the lepton pair forward-backward asymmetry,²³ and the tau polarization asymmetry²⁴ in the case $\ell = \tau$. Measurement of all these quantities would allow for the determination of the sign and magnitude of the Wilson coefficients for the electroweak loop operators and thus provide a completely model independent analysis. We note that measurement of these distributions requires the high statistics samples which will be available at future B-factories. The lepton pair invariant mass distribution for $b \rightarrow se^+e^-$ is displayed in Fig. 3(a) (taking $m_t = 175$ GeV), where the solid curve includes the contributions from the short and long range effects and the dashed curve represents the short distance alone. We see that the long distance contributions dominate only in the $M_{e^+e^-}$ regions near the ψ and ψ' resonances, and observations away from these peaks would cleanly separate the short distance physics. The tau polarization asymmetry is presented in Fig. 3(b); we see that it is large and negative for this value of m_t . As an example of how new physics can affect this process, we examine $b \rightarrow s\ell^+\ell^-$ in the case of an anomalous $WW\gamma$ vertex. The resulting invariant mass spectrum is shown in Fig. 3(c) for several values of $\Delta\kappa_\gamma$ (taking $\lambda_\gamma = 0$), and the variation of the tau polarization asymmetry with non-zero values of $\Delta\kappa_\gamma$ and λ_γ is displayed in Fig. 3(d) for $\hat{s} \equiv q^2/m_b^2 = 0.7$.

5. CP Violation in B Decays

CP violation in the B system will be examined²⁵ during the next decade at dedicated B-Factories. CP violation arises in the SM from the existence of the phase in the 3 generation CKM matrix. The relation $V_{tb}V_{td}^* + V_{cb}V_{cd}^* + V_{ub}V_{ud}^* = 0$, which is required by unitarity, can be depicted as a triangle in the complex plane, where the area of the triangle represents the amount of CP violation. It can be shown that the apex of the triangle is located at the point (ρ, η) in the complex plane, where ρ and η are parameters describing the CKM matrix in the Wolfenstein notation. The present status of these parameters is summarized in Fig. 4(a), where the shaded area is that allowed in the SM. This region is determined by measurements of the quantities (i) $|V_{ub}|$ and $|V_{cb}|$, (ii) ϵ , the CP violation parameter in K_L^0 decay, and (iii) the rate for $B_d^0 - \bar{B}_d^0$ mixing, together with theoretical estimates for the parameters which relate these measurements to the underlying theory, such as B_K , f_B , and B_B . The value of $\bar{m}_t(m_t)$ is taken to be consistent with the physical range 174 ± 16 GeV. This yields the allowed ranges for the angles of the triangle: $-0.89 \leq \sin 2\alpha \leq 1.00$, $0.18 \leq \sin 2\beta \leq 0.81$, and $-1.00 \leq \sin 2\gamma \leq 1.00$.

It is important to remember that this picture can be dramatically altered if new physics is present, even if there are no new sources of CP violation. Figure 4(b) displays the constraints in the $\rho - \eta$ plane in the two-Higgs-doublet Model II. In this case the presence of the extra Higgs doublet is felt by the virtual exchange of the H^\pm boson in the box diagram which mediates $B_d^0 - \bar{B}_d^0$ mixing and governs the value of ϵ . For this $\rho - \eta$ region, the allowed ranges of the angles of the unitarity triangle become

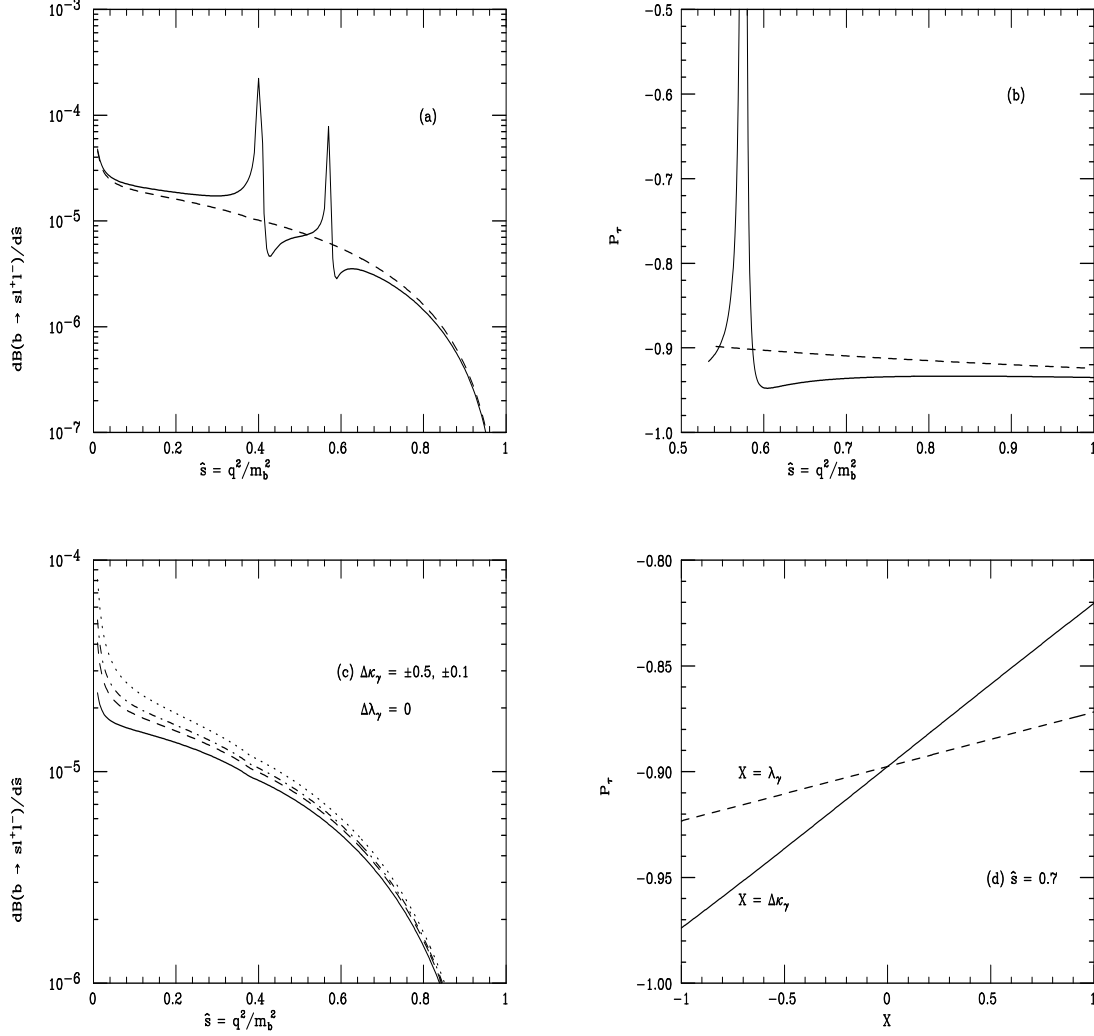


Fig. 3. The (a) lepton pair mass distribution (with $\ell = e$) and (b) tau polarization asymmetry (with $\ell = \tau$) in the SM, and the (c) lepton pair mass distribution and (d) tau polarization asymmetry with anomalous $WW\gamma$ couplings as labeled, for the process $b \rightarrow sl^+l^-$ with $m_t = 175$ GeV.

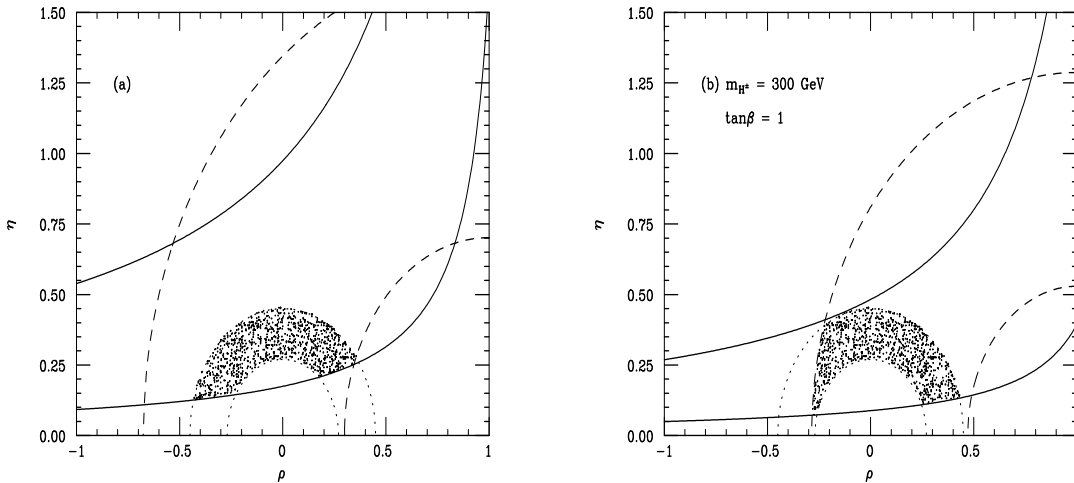


Fig. 4. Constraints in the (a) SM and (b) two-Higgs-doublet Model II in the $\rho - \eta$ plane from $|V_{ub}|/|V_{cb}|$ (dotted circles), $B_d^0 - \bar{B}_d^0$ mixing (dashed circles) and ϵ (solid hyperbolas). The shaded area corresponds to that allowed for the apex of the Unitarity triangle.

$-1.00 \leq \sin 2\alpha \leq 1.00$, $0.12 \leq \sin 2\beta \leq 0.81$, and $-1.00 \leq \sin 2\gamma \leq 1.00$. We see that the SM predictions for CP violation are thus modified.

6. Summary

We have examined several aspects of physics in the B system in a variety of models containing physics beyond the SM and discovered that these processes can provide powerful insights on new interactions. In some cases, such as in $b \rightarrow s\gamma$, constraints are obtained which either complement or are stronger than those from other low-energy processes or from direct collider searches. The decay $b \rightarrow s\ell^+\ell^-$ is also an excellent probe of new physics and we eagerly anticipate its detection. We also await further improvements in the data on $Z \rightarrow b\bar{b}$ to see if this is the process which finally cracks the SM. In summary, we have an exciting decade of B physics ahead!

References

1. D. Schaile, in *27th International Conference on High Energy Physics*, Glasgow, Scotland, July 1994; U. Uwer in *30th Rencontres de Moriond: Electroweak Interactions and Unified Theories*, Meribel les Allures, France, March 1995.
2. F. Abe *et al.*, (CDF Collaboration), FERMILAB-PUB-95-022-E (1995); S. Abachi *et al.*, (D0 Collaboration), FERMILAB-PUB-95-028-E (1995).
3. A.K. Grant, Phys. Rev. **D51**, 207 (1995).
4. The ZFITTER package: D. Bardin *et al.*, Z. Phys. **C44**, 493 (1989); Nucl. Phys. **B351**, 1 (1991); Phys. Lett. **B255**, 290 (1991); CERN Report, CERN-TH-6443/92, 1992.

5. J.F. Gunion, H.E. Haber, G.L. Kane, and S. Dawson, *The Higgs Hunters Guide*, (Addison-Wesley, Redwood City, CA, 1990).
6. A. Djouadi *et al.*, Nucl. Phys. **B349**, 48 (1991); A. Denner *et al.*, Z. Phys. **C51**, 695 (1991); M. Boulware and D. Finnel, Phys. Rev. **D44**, 2054 (1991).
7. J.D. Wells, C. Kolda, and G.L. Kane, Phys. Lett. **B338**, 219 (1994).
8. C.P. Burgess and D. London, Phys. Rev. Lett. **69**, 3428 (1992).
9. K. Hagiwara *et al.*, Nucl. Phys. **B282**, 253 (1987).
10. O.J.P. Eboli, M.C. Gonzalez-Garcia, and S.F. Novaes, Phys. Lett. **B339**, 119 (1994).
11. T.G. Rizzo, Phys. Rev. **D51**, 3811 (1995); G. Kopp *et al.*, Z. Phys. **C65**, 545 (1995).
12. M.S. Alam *et al.*, (CLEO Collaboration), Phys. Rev. Lett. **74**, 2885 (1995).
13. C. Bernard, P. Hsieh, and A. Soni, Phys. Rev. Lett. **72**, 1402 (1994).
14. A.J. Buras *et al.*, Nucl. Phys. **B424**, 374 (1994), and references therein.
15. For a review of implications of non-SM physics in $b \rightarrow s\gamma$, see, J.L. Hewett, in *21st Annual SLAC Summer Institute on Particle Physics*, Stanford, Ca, July 1993.
16. T.G. Rizzo, Phys. Rev. **D38**, 820 (1988); W.-S. Hou and R.S. Willey, Phys. Lett. **B202**, 591 (1988); C.Q. Geng and J.N. Ng, Phys. Rev. **D38**, 2858 (1988); B. Grinstein, R. Springer, and M. Wise, Nucl. Phys. **B339**, 269 (1990); V. Barger, J.L. Hewett, and R.J.N. Phillips, Phys. Rev. **D41**, 3421 (1990).
17. J.L. Hewett, Phys. Rev. Lett. **70**, 1045 (1993); V. Barger, M. Berger, and R.J.N. Phillips, Phys. Rev. Lett. **70**, 1368 (1993).
18. S. Bertolini, *et al.*, Nucl. Phys. **B294**, 321 (1987), and Nucl. Phys. **B353**, 591 (1991); R. Barbiero and G.F. Giudice, Phys. Lett. **B309**, 86 (1993); R. Garisto and J.N. Ng, Phys. Lett. **B315**, 119 (1993); M.A. Diaz, Phys. Lett. **B322**, 207 (1994); F.M. Borzumati Z. Phys. **C63**, 291 (1994); S. Bertolini and F. Vissani, Trieste Report SISSA 40/94/EP; J.L. Lopez *et al.*, Phys. Rev. **D48**, 974 (1993).
19. T. Goto and Y. Okada, KEK Report KEK-TH-421 (1994).
20. T.G. Rizzo, Phys. Lett. **B315**, 471 (1993); S.-P. Chia, Phys. Lett. **B240**, 465 (1990); K.A. Peterson, Phys. Lett. **B282**, 207 (1992).
21. J. Ellison (D0 Collaboration), Proceeding of *1994 Meeting of the Division of Particles and Fields*, Albuquerque, NM (1994). For comparable bounds from CDF and UA2, see F. Abe *et al.*, (CDF Collaboration) Phys. Rev. Lett. **74**, 1936 (1995); J. Alitti *et al.*, UA2 Collaboration, Phys. Lett. **B277**, 194 (1992).
22. N.G. Deshpande and J. Trampetic, Phys. Rev. Lett. **60**, 2583 (1988); C.S. Lim, T. Morozumi, and A.I. Sanda, Phys. Lett. **B218**, 343 (1989); N.G. Deshpande, J. Trampetic, and K. Panrose, Phys. Rev. **D39**, 1461 (1989); B. Grinstein, M.J. Savage, and M.B. Wise, Nucl. Phys. **B319**, 271 (1989).
23. A. Ali, G.F. Giudice, and T. Mannel CERN Report CERN-TH.7346/94; A. Ali, T. Mannel, and T. Morozumi, Phys. Lett. **B273**, 505 (1991).
24. J.L. Hewett, SLAC Report, SLAC-PUB-95-6820.
25. D. Boutigny *et al.*, SLAC Report SLAC-0443 (1994); M.T. Cheng *et al.*, KEK Report KEK-94-02 (1994).